BIOCHEMISTRY
including biophysical chemistry & molecular biology

Article

pubs.acs.org/biochemistry

Understanding FtsZ Assembly: Cues from the Behavior of Its N- and C-Terminal Domains

Bhavya Jindal and Dulal Panda*

Department of Biosciences and Bioengineering, Indian Institute of Technology Bombay, Mumbai 400076, India

Supporting Information

ABSTRACT: FtsZ polymerizes to form a cytokinetic ring at the center of a bacterial cell, which engineers bacterial cell division. FtsZ consists of N-terminal and C-terminal core domains followed by a C-terminal spacer and a conserved C-terminal tail region. Though it has been reported that both N- and C-domains can fold independently, the assembly behaviors of the N- and C-domains are not clear. In this study, we created five truncated constructs of *Bacillus subtilis* FtsZ, two N-domain and three C-domain constructs, and expressed and purified them. We determined their assembly properties and their effect on the assembly of full-length FtsZ to gain insight into the mechanism of FtsZ polymerization. We found that the N-domain of *B. subtilis* FtsZ can polymerize on its own in a GTP-dependent manner. Further, we obtained evidence indicating that the N-domain could bind to GTP but could not hydrolyze GTP by itself. In addition, the N-domain was found to inhibit the assembly of full-length FtsZ. Interestingly, the N-domain was found to enhance the GTPase activity of full-length FtsZ. An analysis of the effects of the N- and C-domains on FtsZ assembly indicated that the assembly of FtsZ might be directional. The work has provided new insight into the assembly characteristics of FtsZ domains and the mechanism of FtsZ polymerization.

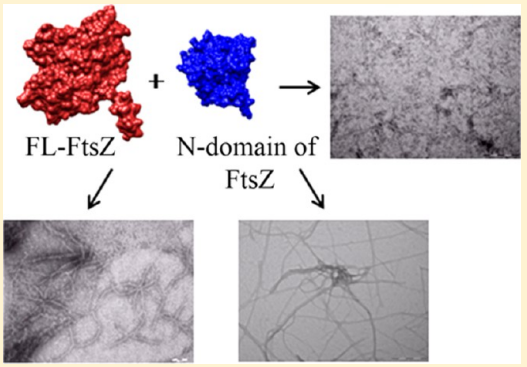

FtsZ, a bacterial cell division protein, polymerizes to form a ring structure at the center of the cells that, in turn, mediates cell division.[1] It is a homologue of the eukaryotic cytoskeletal protein tubulin[2,3] and displays GTPase activity. Like tubulin, it polymerizes in a GTP-dependent manner to form filaments *in vitro*, and the polymers are structurally similar to the tubulin polymers.[4−6] In general, FtsZ forms linear polymers, which are one subunit thick and form structures like sheets, spirals, and rings in the presence of certain additives.[4,6,7] The structure of the Z-ring inside the cells is still not clear, although it has been suggested that the Z-ring is a highly dynamic structure that is made of laterally associated FtsZ protofilaments.[8,9]

The crystal structures of FtsZs from *Methanococcus jannaschii*, *Pseudomonas aeruginosa*, *Bacillus subtilis*, and *Aquifex aeolicus* show that FtsZ consists of two globular domains, an amino-terminal domain and a carboxy-terminal domain, connected by a central helix.[2,10] The N-domain has a Rossman fold, similar to the GTPases like ras and EF-Tu, which binds to GTP. The C-domain core has a chorismate mutase-like fold and a synergy loop (T7) that inserts into the N-domain of the adjacent monomer and brings about GTP hydrolysis.[2,11] The assembly of the FtsZ protofilaments occurs when the N-domain of one FtsZ monomer contacts the C-domain of another FtsZ monomer. The assembly of FtsZ protofilaments is suggested to be directional, with the monomers being added at the bottom interface of the protofilaments.[12,13] Following the C-domain core is a spacer region having a variable length in different bacterial FtsZ forms and a highly conserved segment, which is known to interact with proteins that regulate FtsZ assembly.[14] A recent study has shown that in *B. subtilis* FtsZ, the extreme C-terminus tail region also plays a role in the lateral interactions of FtsZ protofilaments.[15]

It has been shown that N- and C-domains of FtsZ can fold independently.[16] In this study, we made five different truncated constructs of *B. subtilis* FtsZ, namely, two N-terminal core domain constructs and three C-terminal core domain constructs. The two N-domain constructs, N1-FtsZ and N2-FtsZ, constituted amino acids 1−178 and 1−204, respectively. N2-FtsZ has the H7 region additionally, as compared to N1-FtsZ. The three C-domain constructs (C1-FtsZ, C2-FtsZ, and C3-FtsZ) consist of residues 205−366, 176−366, and 176−382, respectively. C1-FtsZ lacks the H7 region, whereas C2-FtsZ includes it; however, both are devoid of the extreme C-terminal tail region of FtsZ. In contrast, C3-FtsZ contains both the H7 region and the C-terminal tail region of FtsZ (Figure 1A). We used these constructs to determine the polymerization properties of the individual FtsZ domains that may provide significant insight into the roles of these domains in FtsZ assembly and assist in the probing of the mechanism of FtsZ polymerization.

We found that the N-domains of FtsZ can polymerize to form filamentous polymers independently in a GTP-dependent manner, whereas the C-domains cannot form polymers on their

Received: February 1, 2013
Revised: August 20, 2013
Published: September 5, 2013

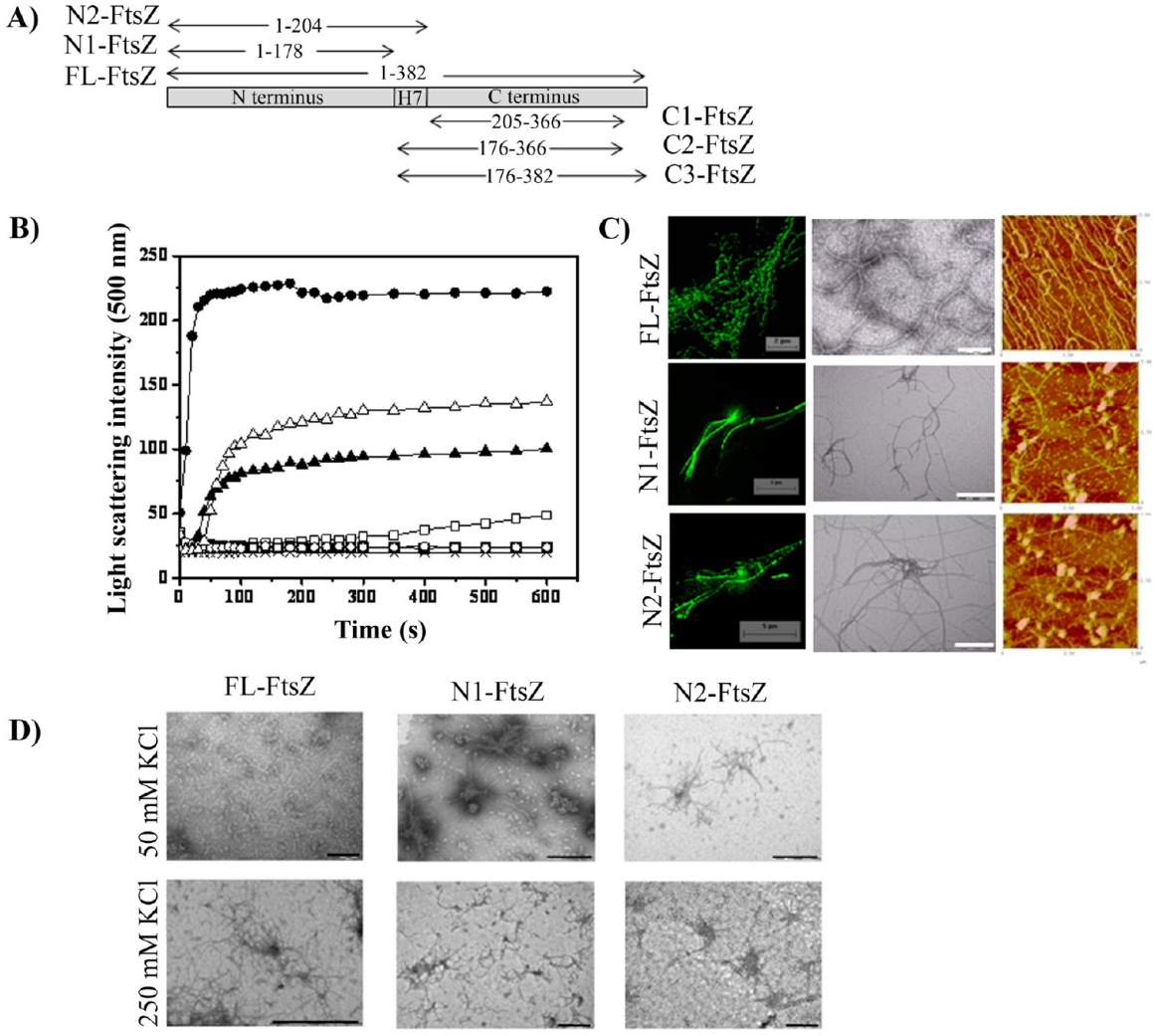

Figure 1. Assembly kinetics of FL-FtsZ and its N-domains and C-domains. (A) Schematic showing the descriptions of the FtsZ constructs used in the study. (B) Light scattering traces showing the polymerization kinetics of 4 μM FL-FtsZ (●), N1-FtsZ (▲), N2-FtsZ (△), C1-FtsZ (□), C2-FtsZ (■), and C3-FtsZ (○). Light scattering by buffer is also denoted (×). (C) Fluorescence images, electron micrographs (scale bar of 200 nm), and atomic force microscopy (AFM) images (x and y axis are 5 μm each) (from left to right, respectively) showing the polymers formed by FL-FtsZ, N1-FtsZ, and N2-FtsZ in 25 mM PIPES buffer containing 50 mM KCl, 5 mM $MgCl_2$ and 1 mM GTP. For fluorescence and electron microscopy, 4 μM protein was used, and for AFM, 1 μM protein was used. (D) Electron microscopic analysis of FL-, N1-, and N2-FtsZ (4 μM each) polymerized in 50 mM HEPES buffer containing 2.5 mM $MgCl_2$, 1 mM GTP, and either 50 or 250 mM KCl. The scale bar is 200 nm.

own. In addition, we found that the N-domain is inhibitory for the assembly of full-length FtsZ (FL-FtsZ) as opposed to the C-domain, which only slightly affected the polymerization of FL-FtsZ. When added to FL-FtsZ, the N-domain increased the GTPase activity, whereas C-domain did not significantly affect the GTPase activity of FL-FtsZ. These observations together indicate that only the N-domain can bind to the FL-FtsZ polymers, supporting the directional assembly of FtsZ.

■ EXPERIMENTAL PROCEDURES

Materials. The polymerase chain reaction (PCR) primers and fluorescein isothiocyanate (FITC) dye were obtained from Sigma (St. Louis, MO). Tetramethylrhodamine-5(6)-isothiocyanate (TRITC) dye was obtained from Invitrogen. Isopropyl β-D-1-thiogalactopyranoside (IPTG) was purchased from Calbiochem. Ni-NTA resin was obtained from Qiagen, and Bio-Gel-P6 resin was purchased from Bio-Rad. All other reagents were of analytical grade and obtained from either Sigma or Himedia (Mumbai, India).

Cloning. We created the following truncated constructs of *B. subtilis* FtsZ: N1-FtsZ (amino acids 1−178), N2-FtsZ (amino acids 1−204), C1-FtsZ (amino acids 205−366), C2-FtsZ (amino acids 176−366), and C3-FtsZ (amino acids 176−382). The following primer pairs were used for the PCR amplification of the regions mentioned above. For the N1 and N2 forms, the forward primer sequence is 5′GGGTTTCATATGTTGGAGTTCGAAAC3′ and the reverse primer sequences are 5′CGCGGATCCTTACGGTGTGTTTTTATC3′ and 5′CGCGGATCCTTAAGGTGTAGCAATC3′, respectively. For the C1−C3 forms, the forward and reverse primer pairs are 5′GGGTTTCATATGGGTCTTATCAACCTT3′ and 5′CGCGGATCCTTAATCAGCCGG3′, 5′GGGTTTCATATGAACACACCGATGCTTGAAGC3′ and 5′CGCGGATCCTTAATCAGCCGGCTGTG3′, and 5′GGGTTTCATATGAACACACCGATGCTTGAAGC3′ and 5′CGCGGATCCTTAGCCGCGTTTATTGC3′, respectively. The N1, N2, C2, and C3 forms were cloned in pET16b, and the C1 form was cloned in pET28a between NdeI and BamHI sites.

dx.doi.org/10.1021/bi400129j | *Biochemistry* 2013, 52, 7071−7081

Protein Purification. *Isolation and Purification of FL-FtsZ and C-Domains.* *B. subtilis* FL-FtsZ,[17] C1-FtsZ, C2-FtsZ, and C3-FtsZ were expressed in *Escherichia coli* BL21(DE3)plysS cells. The cells were grown at 37 °C in Luria-Bertani (LB) medium in the presence of appropriate antibiotics. The cells were then induced at late log phase (OD_{600} ~ 0.8) with 1 mM IPTG for 6 h. Cells were harvested and washed with lysis buffer [50 mM NaH_2PO_4 (pH 8.0) and 300 mM NaCl]. The cell pellet was suspended in ice-cold lysis buffer containing 0.1% β-ME and 2 mM PMSF. Lysozyme (1 mg/mL) was added, and cells were incubated for 1 h on ice. The cells were then disrupted by sonication (10 pulses, 30 s each), and the crude lysate obtained was spun at 88760*g* and 4 °C to obtain a cleared cell lysate. Imidazole (5 mM) was added to the cleared cell lysate to prevent the binding of nonspecific proteins to Ni-NTA. The imidazole-containing supernatant was then mixed with an activated Ni-NTA resin and incubated while being gently shaken for 1 h at 4 °C. This resin was then loaded on a column, and the flow through was collected. The column was extensively washed with buffers containing increasing imidazole concentrations [25 mM PIPES (pH 6.8) and 300 mM NaCl with 25, 50, and 75 mM imidazole]. The proteins were eluted with buffer containing 250 mM imidazole. Protein fractions were pooled and desalted using the Biogel P-6 resin using either 25 mM PIPES buffer (pH 6.8) or 50 mM HEPES buffer (pH 7.5). The pure protein obtained was then concentrated and stored at −80 °C.

Isolation and Purification of N-Domains. N1-FtsZ and N2-FtsZ were expressed in *E. coli* BL21(DE3)plysS and *E. coli* C41, respectively. The *N1-ftsz* transformed BL21(DE3)plysS cells were grown in LB medium in the presence of 100 μg/mL ampicillin and 12.5 μg/mL chloramphenicol, and the *N2-ftsz* transformed C41 cells were grown in LB medium in the presence of 100 μg/mL ampicillin until the OD_{600} reached 0.8−1. Subsequently, the cells were induced with 1 mM IPTG for 6 h and then collected by centrifugation. The cells were lysed using 8 M urea, and the proteins were subsequently refolded during purification using TN buffer.[18−20] Briefly, the cells were lysed in a buffer containing 50 mM Tris-HCl (pH 8.0), 300 mM NaCl, 8 M urea, 0.1% β-ME, 2 mM PMSF, and 1 mg/mL lysozyme. The cells were then disrupted by sonication (10 pulses, 30 s each), and the crude lysate obtained was spun at 88760*g* and 30 °C to gain a cleared cell lysate. Imidazole (5 mM) was added to the cleared cell lysate to prevent nonspecific binding. The imidazole-containing supernatant was then mixed with an activated Ni-NTA resin pre-equilibriated with a buffer containing 50 mM Tris-HCl (pH 8.0), 300 mM NaCl, 8 M urea, and 5 mM imidazole and incubated while being gently shaken for 1 h at room temperature. This resin was then loaded onto a column, and the flow-through was collected. The column was extensively washed with TN buffer [Tris-HCl (pH 8.0) and 150 mM NaCl] and then with an imidazole concentration gradient (25, 50, and 75 mM). The protein was eluted with 250 mM imidazole. The protein fractions were pooled and then desalted using the Biogel P-6 resin using either 25 mM PIPES buffer (pH 6.8) or 50 mM HEPES buffer (pH 7.5). The pure protein obtained was then concentrated and stored at −80 °C.

To check whether N1- and N2-FtsZ were properly folded, we monitored the far-UV circular dichroism spectra (198−260 nm) of FL-, N1-, and N2-FtsZ using a JASCO spectropolarimeter. The spectra were recorded using a quartz cuvette with a path length of 0.1 cm in 10 mM phosphate buffer (pH 7.4) at 25 °C. Each spectrum was an average of three scans. The spectral data were deconvoluted using CDNN from JASCO.[21] The secondary structure contents estimated by the CDNN analysis corroborated those obtained from the sequences of these proteins (Table S1 of the Supporting Information). Secondary structure contents were derived from the sequences using EMBL server.[22,23]

Measurement of GTP Binding. GTP binding was monitored using 2′,3′-*O*-(2,4,6-trinitrocyclohexadienylidine)-guanosine 5′-triphosphate (TNP-GTP), a fluorescent analogue of GTP.[20,24] The proteins (5 μM FL-, N1-, and N2-FtsZ) were incubated without and with 250 μM GTP in 25 mM PIPES buffer (pH 6.8) containing 5 mM $MgCl_2$, 300 mM NaCl, and 10% glycerol and incubated for 1 h on ice. Then, the reaction mixtures were further incubated with 15 μM TNP-GTP for 1 h on ice. The emission spectra of the samples were monitored from 500 to 600 nm using an excitation wavelength of 410 nm.

Labeling of Proteins with FITC and TRITC. FITC labeling of proteins was conducted by incubating the proteins with a 10-fold molar excess of FITC for 4 h on ice. The labeling reaction was quenched by adding 10 mM Tris-HCl buffer (pH 8.0). The unbound dye molecules were removed by passing the mixture through a gel filtration (Bio-Gel P-4 resin) column followed by dialysis against 25 mM PIPES buffer (pH 6.8) for 4 h at 4 °C. The concentration of proteins was measured by the Bradford assay.[25] The incorporation ratio of FITC per monomer was estimated to be 0.6−0.7 per monomer for the proteins. N2-FtsZ was covalently modified with TRITC as described above. N2-FtsZ was incubated with a 5-fold molar excess of TRITC with respect to the protein for 8 h on ice, and the unbound dye was removed as described above.

Light Scattering Assay. The polymerization of proteins was assessed by 90° light scattering using a JASCO 6500 spectrofluorometer. Different constructs of FtsZ were polymerized in 25 mM PIPES buffer (pH 6.8) containing 50 mM KCl and 5 mM $MgCl_2$ in the presence of 1 mM GTP. The reaction mixture was immediately transferred into a quartz cuvette for monitoring the light scattering signal at 37 °C for 10 min at 500 nm.[26] The initial rates of polymerization of the different FtsZ constructs were determined from the slope of the scattering signal for the initial 90 s of the assembly.

Sedimentation Assay. The protein mixtures were prepared in 25 mM PIPES (pH 6.8) and 50 mM KCl and incubated for 20 min on ice. Then 5 mM $MgCl_2$ and 1 mM GTP were added to the reaction mixtures and polymerized for 10 min at 37 °C. Polymers were sedimented at 127814*g* for 20 min at 30 °C. The supernatant was decanted carefully without disturbing the pellet. The pellet was dissolved and loaded on sodium dodecyl sulfate−polyacrylamide gel electrophoresis (SDS−PAGE) gel. The protein concentration of the pellet was estimated from the SDS−PAGE gel stained with Coomassie brilliant blue R using ImageJ.

Determination of the Critical Concentration for the Assembly of FtsZ Variants. The critical concentration of FL-FtsZ and N2-FtsZ was determined by sedimentation as described previously.[27] Briefly, different concentrations of proteins (2, 3, 4, 5, and 6 μM FL-FtsZ and 1, 2, 3, 4, 5, and 6 μM N2-FtsZ) were polymerized in 25 mM PIPES buffer (pH 6.8) in the presence of 50 mM KCl, 5 mM $MgCl_2$, and 1 mM GTP at 37 °C for 10 min. Polymers were collected through sedimentation (127814*g*) for 20 min at 30 °C. The protein concentration in the supernatant was determined using a Bradford assay. Subsequently, the amount of protein

dx.doi.org/10.1021/bi400129j | *Biochemistry* 2013, 52, 7071−7081

polymerized was estimated by subtracting the concentration of protein in the supernatant from the total protein concentration. Similarly, the critical concentration for the polymerization of both FL-FtsZ and N2-FtsZ was determined in 50 mM HEPES buffer (pH 7.5) in the presence of 50 mM KCl, 2.5 mM $MgCl_2$, and 1 mM GTP.

GTPase Assay. Protein samples were prepared in 25 mM PIPES buffer (pH 6.8) containing 50 mM KCl and 5 mM $MgCl_2$. Then, 1 mM GTP was added to the mixtures, and the mixtures were kept at 37 °C for polymerization. An aliquot of 40 μL was taken at different time points (0, 2, 5, 10, and 15 min); the reaction was quenched by adding 10% (v/v) perchloric acid, and the samples were kept on ice. All the samples were taken; 900 μL of ammonium-molybdate malachite green was added to the reaction mixtures, and they were incubated in the dark for 30 min. The absorbance of the samples was measured at 650 nm, and the amount of P_i released was determined using a phosphate standard curve.[26,28]

Electron Microscopy. Protein samples (4 μM FL-, N1-, and N2-FtsZ) were prepared in 25 mM PIPES buffer (pH 6.8) and 50 mM KCl. Then 5 mM $MgCl_2$ and 1 mM GTP were added, and the proteins were allowed to polymerize when the samples were placed in a 37 °C water bath for 5 min. Then, the samples were adsorbed on Formvar carbon-coated copper grids and subjected to negative staining using a 2% uranyl acetate solution for 45−60 s. The samples were analyzed using an FEI Tecnai-G^2 12 electron microscope (Philips). The polymerization of FL-, N1-, and N2-FtsZ was also monitored in 50 mM HEPES buffer (pH 7.5) containing 2.5 mM $MgCl_2$ with 50 and 250 mM KCl.

Atomic Force Microscopy. Proteins (1 μM) were taken in 25 mM PIPES buffer (pH 6.8) and 50 mM KCl and polymerized in the presence of 5 mM $MgCl_2$ and 1 mM GTP at 37 °C for 10 min. An aliquot (10 μL) of the sample was placed on a mica sheet (2 mm × 2 mm) and dried. The images were acquired in the tapping mode using the digital instruments multimode nanoscope IV scanning probe microscope.

Fluorescence Microscopy. Protein samples (using 4 μM labeled proteins) were prepared in 25 mM PIPES buffer (pH 6.8) and 50 mM KCl, and then 5 mM $MgCl_2$ and 1 mM GTP were added. Polymerization was conducted at 37 °C for 10 min. The samples were then placed on clean glass slides, covered with glass coverslips, and observed using a fluorescence microscope (Eclipse TE2000-U, Nikon, Tokyo, Japan). The images were captured using a Cool SNAP-Pro camera and processed using Image-Pro Plus version 5.0.

Colocalization Assay. FITC-labeled FtsZ (9 μM) was polymerized in 50 mM HEPES buffer (pH 7.5), 50 mM KCl, 2.5 mM $MgCl_2$, and 1 mM GTP at 37 °C for 2 min; 150 nM TRITC-labeled N2-FtsZ was then added to this mixture and further polymerized for 4 min. The sample was then placed on a clean glass slide (24 mm × 60 mm) and covered with another glass coverslip (24 mm × 24 mm). The sample was immediately visualized using a fluorescence microscope (Eclipse TE2000-U, Nikon) under an FITC filter and a TRITC filter. Similarly, the only FITC-FtsZ was polymerized and observed under FITC and TRITC filters. The assay was also performed using 3 μM FITC-labeled FtsZ and 60 nM TRITC-labeled N2-FtsZ in 25 mM PIPES buffer (pH 6.8) containing 50 mM KCl, 5 mM $MgCl_2$, and 1 mM GTP.

N-Domain Model Building. The three-dimensional (3D) coordinates for the structure of *B. subtilis* FtsZ were obtained from Protein Data Bank (PDB) entry 2VXY.[29,30] To obtain the structure of the N-domain, the coordinates for amino acids 11−204 were kept and the rest of the coordinates were deleted. Docking of the N-domain versus the N-domain was performed using Patchdock.[31,32] The obtained complexes were energy minimized using spdbv viewer.[33] The lowest-energy complex was taken, and the 3D structure of the N-domain filament was built from this dimer using the pair fitting module of PyMol.[34] The residues involved in the interactions (hydrophobic and H-bonding interactions) between the two chains of the N-domain dimer were determined using Naccess[35] and UCSF Chimera.[36] The figures have been rendered in UCSF Chimera.[36]

RESULTS

N-Domains of FtsZ Polymerized To Form Filaments, whereas C-Domains Did Not Polymerize. C-Domains of FtsZ did not show any increase in light scattering, indicating that C-domain constructs do not polymerize independently (Figure 1B). Interestingly, both N1- and N2-FtsZ showed an increase in light scattering in the presence of GTP, indicating that the N-domains of FtsZ might polymerize alone (Figure 1B). However, the rate and extent of polymerization of N-domains were lower than those of FL-FtsZ. For example, the initial rates (measured for 90 s) of polymerization of FL-FtsZ, N1-FtsZ, and N2-FtsZ were found to be 55, 8, and 10 units/s, respectively.

The assembly of N-domains was further probed by electron microscopy, fluorescence microscopy, and atomic force microscopy (Figure 1C). Long thin filaments were observed under an electron microscope in case of both N1- and N2-FtsZ. In addition, atomic force microscopic analysis showed that FL-FtsZ formed very long filaments, whereas N-domains formed relatively shorter polymers than FL-FtsZ (Figure 1C).

To analyze the polymerization of N1- and N2-FtsZ under different solution conditions, the assembly of FL-, N1-, and N2-FtsZ was also monitored in HEPES buffer (pH 7.5) in the presence of two different concentrations (50 and 250 mM) of KCl. Under these conditions, N1- and N2-FtsZ were also found to form polymers (Figure 1D). However, the polymers were found to be shorter and thinner in HEPES buffer than those formed in PIPES buffer.

FL-, N1-, and N2-FtsZ contain an N-terminal six-His tag; therefore, the polymerization of these proteins was also observed after removing the His tag using Factor Xa. The His tag cleaved proteins were also found to polymerize efficiently (Figure S1 of the Supporting Information). Because proteins without and with the His tag exhibited similar assembly properties, we used proteins with the His tag for the rest of the experiments.

The critical concentrations for polymerization of FL-FtsZ and N2-FtsZ were determined in both PIPES and HEPES buffers (Figure 2). The critical concentrations for polymerization of FL-FtsZ and N2-FtsZ were determined to be 0.9 ± 0.14 and 0.3 ± 0.08 μM, respectively, in PIPES buffer, suggesting that N2-FtsZ polymerized with a critical concentration that was lower than that of FL-FtsZ (Figure 2A,B). The critical concentrations for polymerization of FL-FtsZ and N2-FtsZ in HEPES buffer were determined to be 1.4 ± 0.20 and 0.6 ± 0.06 μM, respectively (Figure 2A,B).

Because the N-domain of FtsZ contains the GTP binding domain, the GTP binding ability of N1- and N2-FtsZ was examined using TNP-GTP, a fluorescent GTP analogue. Both N1 and N2 constructs were found to bind to TNP-GTP, and GTP was able to inhibit the binding of TNP-GTP to these

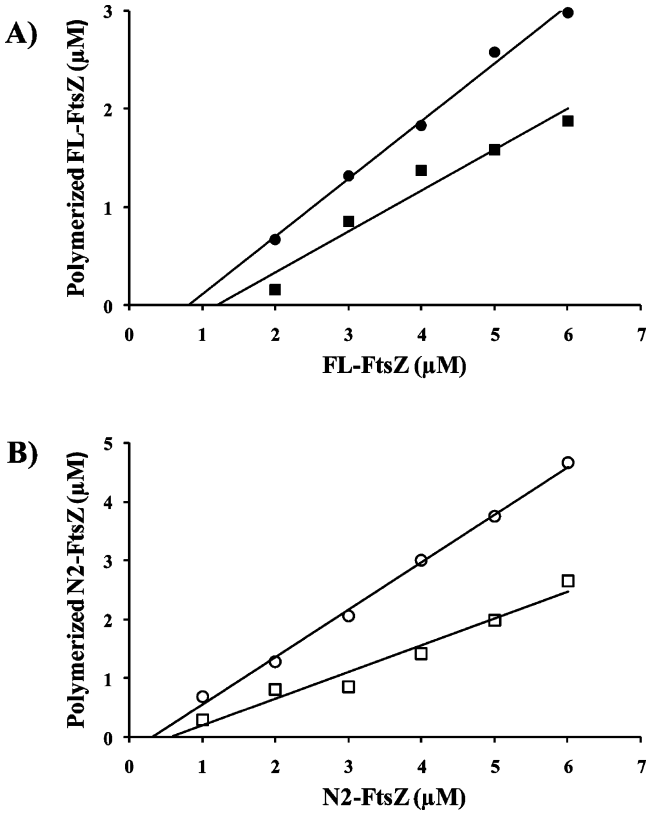

Figure 2. Critical concentrations of FL-FtsZ and N2-FtsZ. The critical concentrations of (A) FL-FtsZ in PIPES (●) and HEPES (■) buffer and (B) N2-FtsZ in PIPES (○) and HEPES (□) buffer were determined by polymerizing different concentrations of FL-FtsZ and N2-FtsZ.

constructs (Figure 3). To check whether the polymerization of N-domains is dependent on GDP or GTP, the polymerization

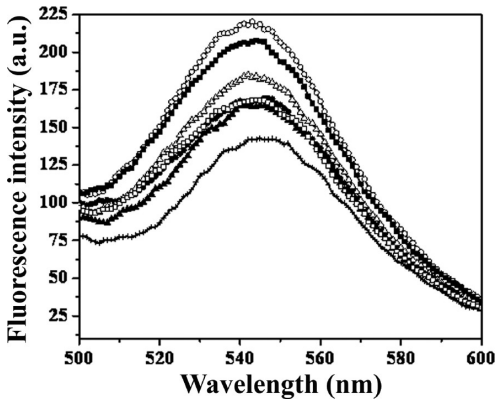

Figure 3. FL-, N1-, and N2-FtsZ bound to TNP-GTP. The fluorescence spectra of TNP-GTP in buffer (×) and in the presence of FL-FtsZ (○), N1-FtsZ (△), and N2-FtsZ (■) are shown. Also, GTP caused a reduction in the increase in fluorescence caused by binding of TNP-GTP to FL-FtsZ (●), N1-FtsZ (▲), and N2-FtsZ (□). The experiment was performed three times.

of N-domains was conducted in the absence and presence of GDP and GTP. The scattering of light was observed in all three cases, in the absence of GDP and GTP, in the presence of GDP, and in the presence of GTP (Figure 4A–C). Further, in the absence of GDP and GTP, only aggregates are visible, whereas polymers are formed in the presence of either GDP or GTP (Figure 4D). Therefore, the increase in light scattering observed in the absence of GDP and GTP is due to the formation of aggregates. Moreover, the morphologies of polymers formed in the presence of GDP and GTP were found to be different; the polymers formed in the presence of GDP are visibly shorter than the polymers formed in the presence of GTP (Figure 4D). FL-FtsZ also formed polymers of different morphologies in the presence of GTP and GDP. The polymers formed in the presence of GTP are longer and thicker, whereas the polymers formed in the presence of GDP appeared to be comparatively shorter and thinner than those formed in the presence of GTP. In addition, the rates of assembly of FL-FtsZ, N1-FtsZ, and N2-FtsZ were higher in the presence of GTP than that of GDP (Figure 4A and insets of Figure 4B,C).

N-Domains Inhibited the Polymerization of FL-FtsZ. The addition of N-domains to FL-FtsZ resulted in the inhibition of polymerization of FL-FtsZ as indicated by light scattering and a sedimentation assay (Figure 5A–C). Electron microscopy and fluorescence microscopic analysis also indicated that the extent of polymer formation decreased in the presence of N-domains (Figure 5D). Electron microscopy showed an overall reduction in the level of polymers in the presence of N-domains, which could be either of FL-FtsZ, N-domains, or both. To specifically probe the status of the assembly of FL-FtsZ, the effect of N-domains on the polymerization of FITC-labeled FL-FtsZ was examined. The number of FITC-labeled FL-FtsZ polymers per field of view was found to be visibly reduced in the presence of N-domains. N2-FtsZ inhibited the polymerization much more efficiently than N1-FtsZ (Figure 5). For instance, the addition of 4 μM N1- and N2-FtsZ reduced the polymerized amount of FL-FtsZ (4 μM) by 13 ± 5 and 49 ± 11%, respectively (Figure 5C). In addition, the inhibition of FL-FtsZ polymerization by N2-FtsZ was monitored in both PIPES and HEPES buffer, and N2-FtsZ inhibited the polymerization of FL-FtsZ in both buffers with similar efficacies (Figure S2 of the Supporting Information). For example, 3 μM N2-FtsZ inhibited the polymerization of 6 μM FtsZ by 28 and 36% in PIPES and HEPES buffers, respectively (Figure S2 of the Supporting Information).

The effect of the N2-domain on the polymerization of FL-FtsZ was also monitored in the presence of different concentrations of GTP. In the presence of 0.1, 0.5, and 2 mM GTP, N2-FtsZ inhibited the polymerization of FL-FtsZ by 40, 46, and 52%, respectively, suggesting that it can effectively inhibit the assembly of FtsZ over a wider range of GTP concentrations (Figure S3 of the Supporting Information), indicating that the inhibition is not caused by depleting the available GTP pool.

The N-Domain Increased the GTPase Activity of FL-FtsZ. The effect of N-domains on the GTPase activity of FL-FtsZ was probed to understand the mechanism by which N1- and N2-FtsZ inhibited the assembly of FL-FtsZ. N-Domains did not show any GTPase activity on their own. However, they increased the GTPase activity of FL-FtsZ. The GTPase activity of FL-FtsZ was significantly higher in the presence of N2-FtsZ than in its absence, while N1-FtsZ could not considerably increase the GTPase activity of FL-FtsZ. Without both N1-FtsZ and N2-FtsZ and with N1-FtsZ and N2-FtsZ, the rates of GTP hydrolysis were found to be 1.9 ± 0.7, 2.1 ± 0.7 (p = 0.652), and 6.3 ± 1.1 (p = 0.004) mol of P_i released (mol of FtsZ)$^{-1}$ min^{-1}, respectively (Figure 5E).

dx.doi.org/10.1021/bi400129j | *Biochemistry* 2013, 52, 7071–7081

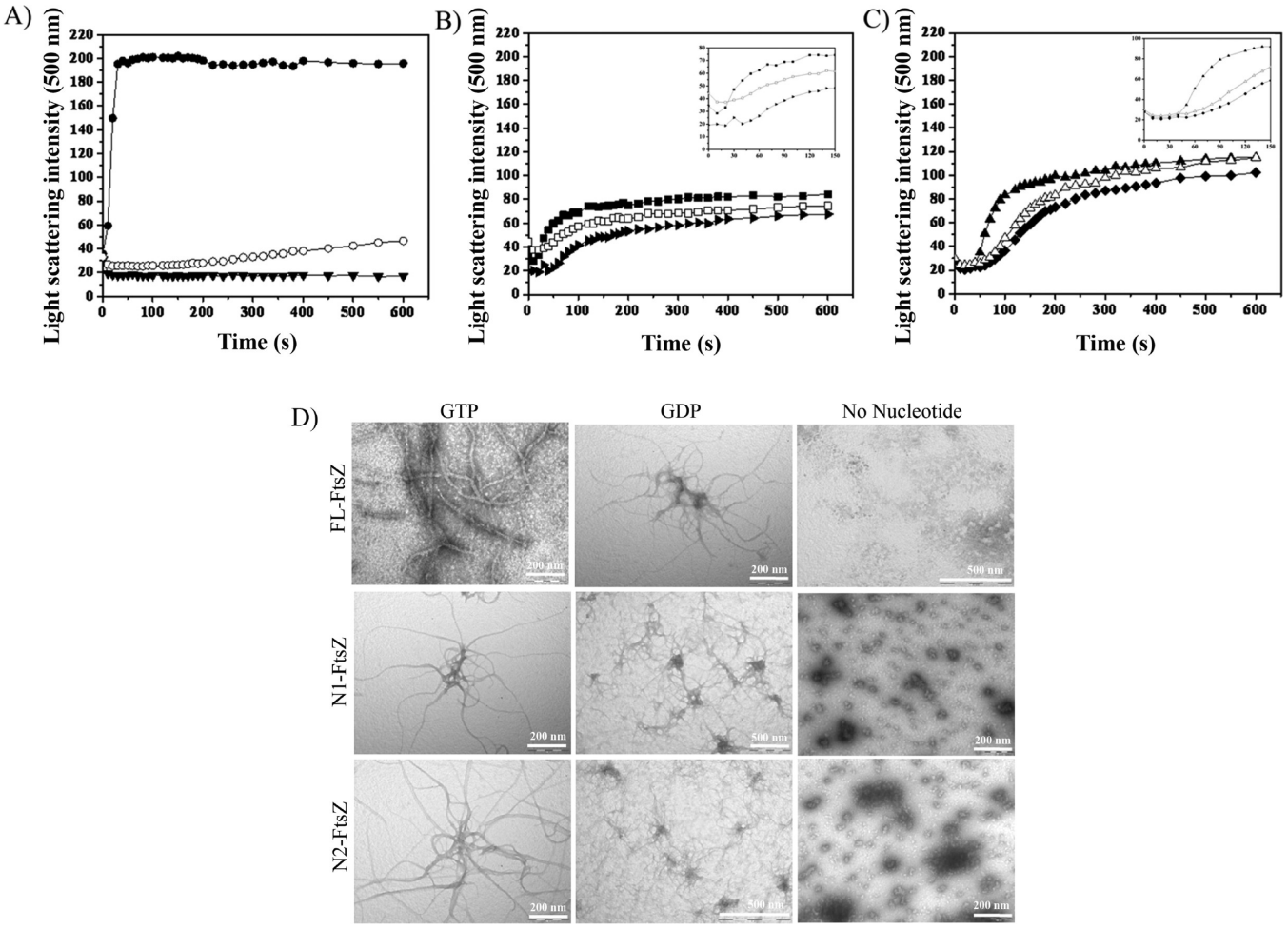

Figure 4. Polymerization of FL-FtsZ and N-domains of FtsZ in the absence and presence of GTP and GDP. The assembly kinetics of 4 μM (A) FL-FtsZ in the absence (▼) and presence of GDP (○) and GTP (●), (B) N1-FtsZ in the absence (▶) and presence of GDP (□) and GTP (■), and (C) N2-FtsZ in the absence (◆) and presence of GDP (△) and GTP (▲) are shown. Insets of panels B and C show the assembly of N1- and N2-FtsZ in the initial 150 s. (D) Electron micrographs showing the polymers of FL-FtsZ, N1-FtsZ, and N2-FtsZ in the absence and presence of GDP and GTP.

C-Domains Inhibited the Polymerization of FL-FtsZ. At equimolar concentrations, the C-domain constructs did not significantly affect the polymerization of FL-FtsZ. However, at 1:2 ratios of FL-FtsZ and C-domain, C-domains were found to inhibit the polymerization of FL-FtsZ (Figure 6A,B). A light scattering assay showed a decrease in both the rate and extent of polymerization of FL-FtsZ in the presence of C-domains. In the sedimentation assay, at 8 μM, C1-FtsZ, C2-FtsZ, and C3-FtsZ inhibited the polymerization of 4 μM FL-FtsZ by 10 ± 3, 19 ± 5, and 34 ± 8%, respectively, suggesting C1-FtsZ, C2-FtsZ, and C3-FtsZ inhibited the assembly of FL-FtsZ with different efficacies (Figure 6B). This might be due to the presence of helix H7 in C2-FtsZ and the presence of both helix H7 and the C-terminal tail in C3-FtsZ.

C-Domains Did Not Significantly Affect the GTPase Activity of FL-FtsZ. In the absence and presence of C1-FtsZ, C2-FtsZ, and C3-FtsZ, the rates of GTP hydrolysis of FL-FtsZ were found to be 1.9 ± 0.3, 1.8 ± 0.3, 1.9 ± 0.4, and 1.7 ± 0.3, respectively, showing that C-domains did not alter the GTPase activity of FL-FtsZ significantly even at a 1:2 FL-FtsZ:C-domain ratio.

N-Domain of FtsZ Localized with FL-FtsZ Protofilaments. Using FITC-labeled FL-FtsZ and TRITC-labeled N2-FtsZ, the binding of the N-domain of FtsZ with the polymers of FL-FtsZ was monitored by fluorescence microscopy. TRITC-labeled N2-FtsZ was found to be localized with the FITC-labeled FL-FtsZ filaments (Figure 7). Similar to the colocalization of TRITC-labeled N2-FtsZ and FITC-labeled FL-FtsZ filaments in HEPES buffer, TRITC-labeled N2-FtsZ was also found to be associated along the length of FITC-labeled FL-FtsZ filaments when the experiment was performed in the PIPES buffer (Figure S4 of the Supporting Information).

3D Models for the FL-FtsZ and N-Domain Polymers. The modeled FL-FtsZ protofilament from the available dimeric structure of FtsZ (*Methanocaldococcus jannaschii*)[16] showed a straight conformation (Figure 8A). We also constructed a 3D model for the N-domain polymers to gain an idea about how the N-domain forms polymers. The 3D model of N-domain filaments displayed a slightly curved structure (Figure 8B and inset 1). Both hydrophobic and H-bonding (Figure 8B, inset 2) interactions were found to be involved in the interaction of N-domains.

■ DISCUSSION

The N-Domain of FtsZ Shows Polymerizing Behavior. The N-domain (the GTP binding domain) of FtsZ was found

dx.doi.org/10.1021/bi400129j | *Biochemistry* 2013, 52, 7071−7081

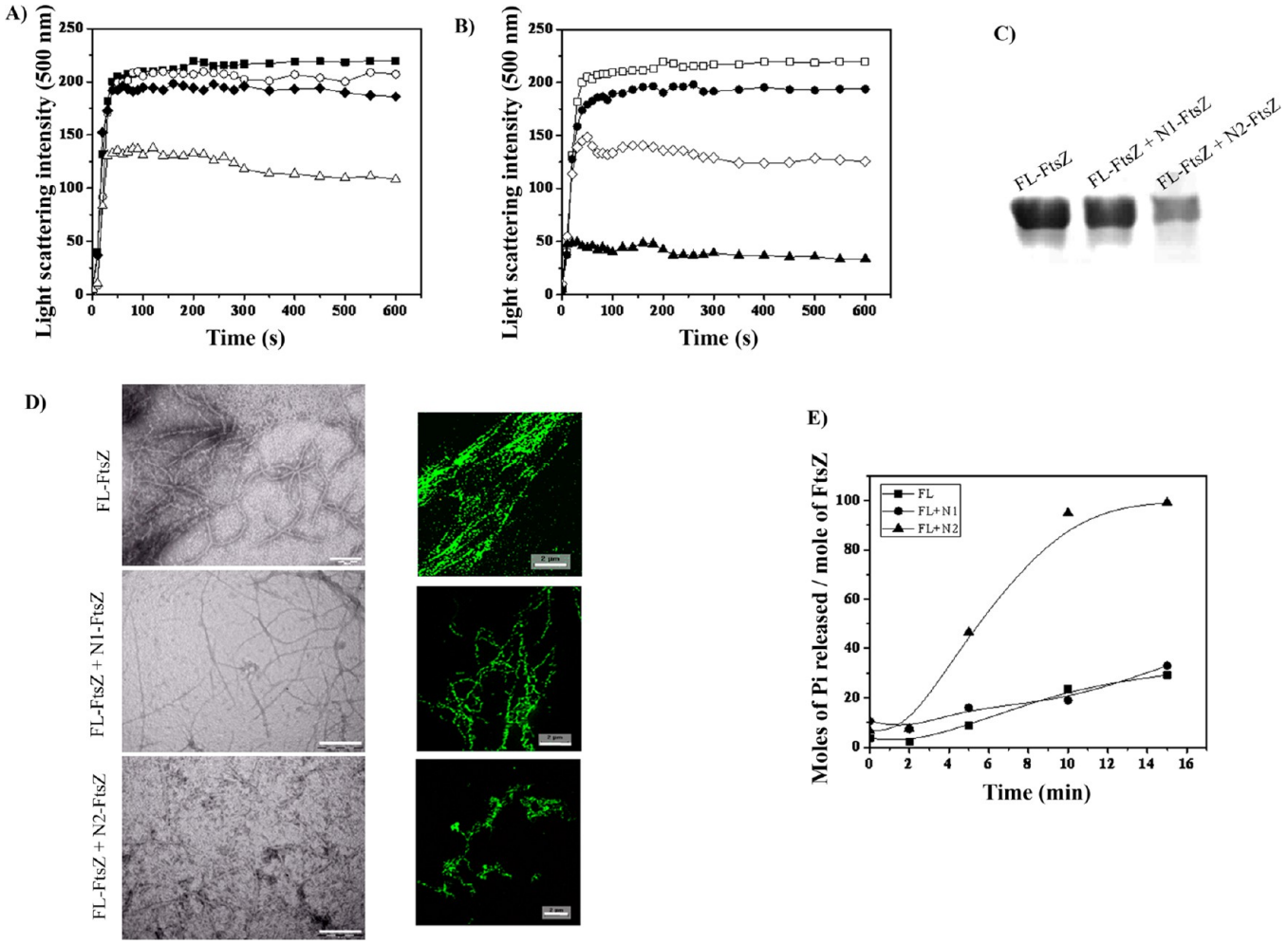

Figure 5. Effects of N-domains on the assembly and GTPase activity of FL-FtsZ. Effects of N1-FtsZ and N2-FtsZ on the polymerization kinetics of FL-FtsZ (4 μM) (A) in the absence (■) and presence of 2 (○), 4 (◆), and 8 μM (△) N1-FtsZ and (B) in the absence (□) and presence of 2 (●), 4 (◇), and 8 μM (▲) N2-FtsZ. (C) N1-FtsZ and N2-FtsZ reduced the amount of polymerized FL-FtsZ. The amount of FL-FtsZ polymerized in the absence and presence of N1- and N2-FtsZ was estimated from the Coomassie blue-stained gel, and the percentage decrease in the amount of polymerized FL-FtsZ was calculated. One of the three sets of experiments is shown. (D) Electron microscopy (the scale bar is 200 nm) and fluorescence microscopy (the scale bar is 2 μm) images showing a decrease in the amount of filamentous polymers of FL-FtsZ in the presence of N1- and N2-FtsZ. (E) GTPase activity of FL-FtsZ in the absence (■) and presence of N1-FtsZ (●) and N2-FtsZ (▲). One of the three sets of experiments is shown.

to assemble to form filamentous polymers in the presence of GTP as well as GDP, while in the absence of GTP and GDP, aggregates of N-FtsZ were formed. It is well established that tubulin, a eukaryotic homologue of FtsZ, exists as an $\alpha\beta$ heterodimer and these heterodimers associate in a GTP-dependent manner to form microtubules.[37] However, the purified β-subunit of tubulin has been shown to polymerize in a manner independent of the α-subunit to form various kinds of structures like filaments, sheets, rings, etc.[38] Similarly, we found that only the N-domain of FtsZ could polymerize to form filaments even in the absence of the C-domain, indicating that the N-domain of FtsZ behaved like the β-subunit of tubulin.[38] Similar to FL-FtsZ, the N-domain of FtsZ was also found to polymerize with a critical concentration suggesting that the assembly of the N-domain also involves nucleation steps. However, the critical concentration for the polymerization of the N-domain was found to be lower than that of FL-FtsZ, indicating that the size of the nucleus was smaller for the N-domain than for FL-FtsZ (Figure 2). The extents of polymerization and bundling were higher in FL-FtsZ than in the N-domains, suggesting that the lateral interactions are predominant in FL-FtsZ polymers (Figure 1).

In a study performed with the N- and C-domains of *Thermotoga martima* (thermophile) FtsZ, it was found that these domains individually could not form any polymers and the combination of the two domains resulted in the formation of filaments like FL-FtsZ but with differences in morphology.[16] Further, the *T. maritima* FtsZ domains when mixed together could hydrolyze GTP, although to a lesser extent than FL-FtsZ.[16] In this study, none of the five *B. subtilis* FtsZ domains exhibited GTPase activity individually. In addition, we also did not find any GTPase activity even after mixing the N- and C-domains. Moreover, the addition of C-domains inhibited the assembly of N-domains (Figure S5 of the Supporting Information). This is most likely due to a minor loss of the proper conformation of the N-domain and/or C-domain upon separation, resulting in the nonfunctional interaction of the two domains (Figure S6 of the Supporting Information). Differences in the polymerization behavior of the two domains in this

dx.doi.org/10.1021/bi400129j | *Biochemistry* 2013, 52, 7071−7081

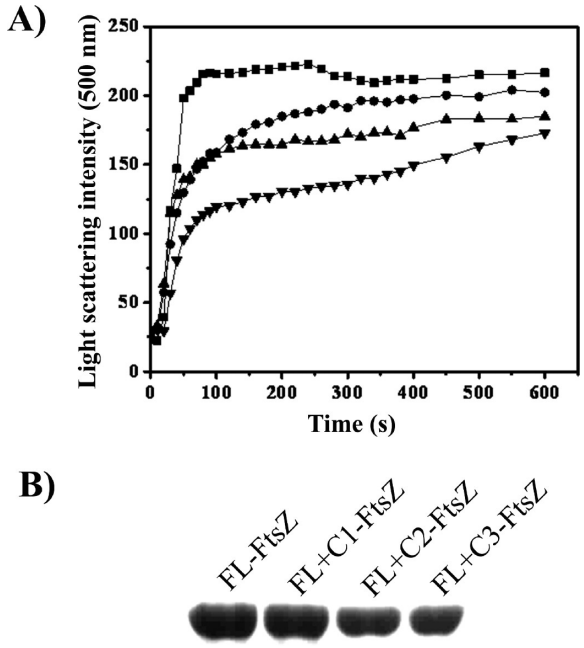

Figure 6. Effects of C-domains on the assembly of FL-FtsZ. (A) Polymerization kinetics of FL-FtsZ (4 μM) in the absence (■) and presence of 8 μM C1-FtsZ (●), C2-FtsZ (▲), and C3-FtsZ (▼). (B) C-Domains reduced the amount of polymerized FL-FtsZ. The amount of FL-FtsZ polymerized in the absence and presence of C1-FtsZ, C2-FtsZ, and C3-FtsZ was estimated from a Coomassie blue-stained gel, and the percentage decrease in the amount of polymerized FL-FtsZ was calculated. The experiment was performed three times independently.

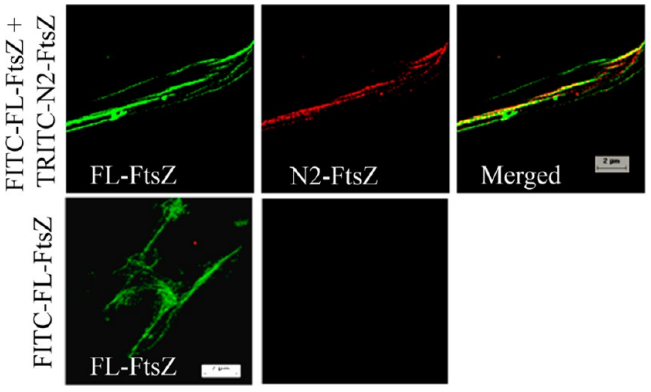

Figure 7. N2-FtsZ localized with the FL-FtsZ filament. FITC-labeled FL-FtsZ (9 μM, green) was polymerized in the presence of 150 nM TRITC-labeled N2-FtsZ (red) in the presence of 50 mM HEPES buffer (pH 7.5), 50 mM KCl, 2.5 mM $MgCl_2$, and 1 mM GTP. TRITC-labeled N2-FtsZ colocalized with the FL-FtsZ protofilament (top). FITC-labeled FL-FtsZ polymers (green) in the absence of TRITC-labeled N2-FtsZ are shown in the bottom panel. The scale bar is 2 μm.

study and the previous study may be due to the origin of FtsZ, which is *B. subtilis* and *T. maritima*, respectively.

The results suggested that the N-domain is sufficient on its own to polymerize and to form filamentous structures, but these polymers may not have any dynamicity because the N-domain cannot hydrolyze GTP on its own. It might be possible that the C-domain contributes to the dynamics of FL-FtsZ filaments, when it is part of the folded protein, and the polymers therefore undergo the states of polymerization and depolymerization. Because both polymerization and depolymerization are crucial for the functionality of FtsZ, FtsZ might have evolved in such a way that the N-domain acquired the C-terminal GTPase activating region to gain the depolymerization function. For cell division to happen, the depolymerization of the ring is required for the final splitting of the daughter cells.[39] However, further experiments are required to confirm the precise roles of these domains in FtsZ.

Recently, two new proteins, FtsZl1 and FtsZl2, of the FtsZ-tubulin superfamily have been identified in bacteria. Sequence analyses of these proteins revealed that the N-domain of these proteins was similar to FtsZ while the C-terminal domain is dissimilar to that of FtsZ,[40] indicating a common N-domain ancestor for FtsZ-tubulin-like family proteins. The polymerization capability of these new families of proteins is still unknown; however, if they do polymerize, then their mechanism might be different as the C-domain region of these families is different from those of the other FtsZ families.

Helix H7 Might Be Important for the Functionality of the N-Domain. N2-FtsZ was found to be much more effective in inhibiting FL-FtsZ polymerization than N1-FtsZ. This striking difference in the effect of these two constructs can be attributed to the absence and presence of helix H7 in N1-FtsZ and N2-FtsZ, respectively. Different groups have placed helix H7 differently with respect to N- and C-domains. Oliva et al. placed helix H7 in the C-domain in *T. maritima* FtsZ,[16] whereas Osawa and Erickson suggested that half of helix H7 belongs to the N-domain of FtsZ and the other half is a component of the C-domain.[13] Our observations suggested that helix H7 might be an integral component of the N-domain and plays an important role in the interaction between the monomers. For this reason, N2-FtsZ could interact more competently to FL-FtsZ and inhibited its assembly as compared to N1-FtsZ.

The Results Support the Directional Polymerization of FtsZ. The addition of the N-domain to FL-FtsZ inhibited the polymerization of FL-FtsZ (Figure 5 and Figure S2 of the Supporting Information). The inhibition of FtsZ assembly can be either due to the sequestration of FtsZ monomers by the N-domain or due to the obstruction of the growth of FtsZ filaments by the binding of the N-domain to the growing FtsZ polymers. If the inhibition would have been by sequestration, then one would expect the GTPase activity of FL-FtsZ to decrease upon addition of the N-domains, but our results showed that N2-FtsZ significantly increased the GTPase activity of FL-FtsZ (Figure 5E). On the other hand, if N-domains inhibited the polymerization by binding to the polymers, then it would cause a decrease in the amount of assembled FL-FtsZ polymers upon addition after the assembly of FL-FtsZ. In support of this idea, we observed that N2-FtsZ inhibited the polymerization of FL-FtsZ even when it was added after the polymerization of FL-FtsZ reached saturation, although the extent is lower compared to the case in which N2-FtsZ was added before the assembly. When N2-FtsZ was added to the reaction mixture before FL-FtsZ had been subjected to polymerization, the polymerization was inhibited by 51 ± 5.7%, whereas when it was added after FL-FtsZ had been polymerized for 5 min, it inhibited the polymerization by 30.6 ± 6.6% (Figure S7 of the Supporting Information). In addition, the colocalization experiment suggested that N2-FtsZ may become incorporated into the FL-FtsZ polymers (Figure 7). This clearly raises the possibility that it would be interacting with FL-FtsZ polymers and reducing its level of polymerization. It is possible that the binding of N2-FtsZ to the growing FtsZ polymers

dx.doi.org/10.1021/bi400129j | *Biochemistry* 2013, 52, 7071−7081

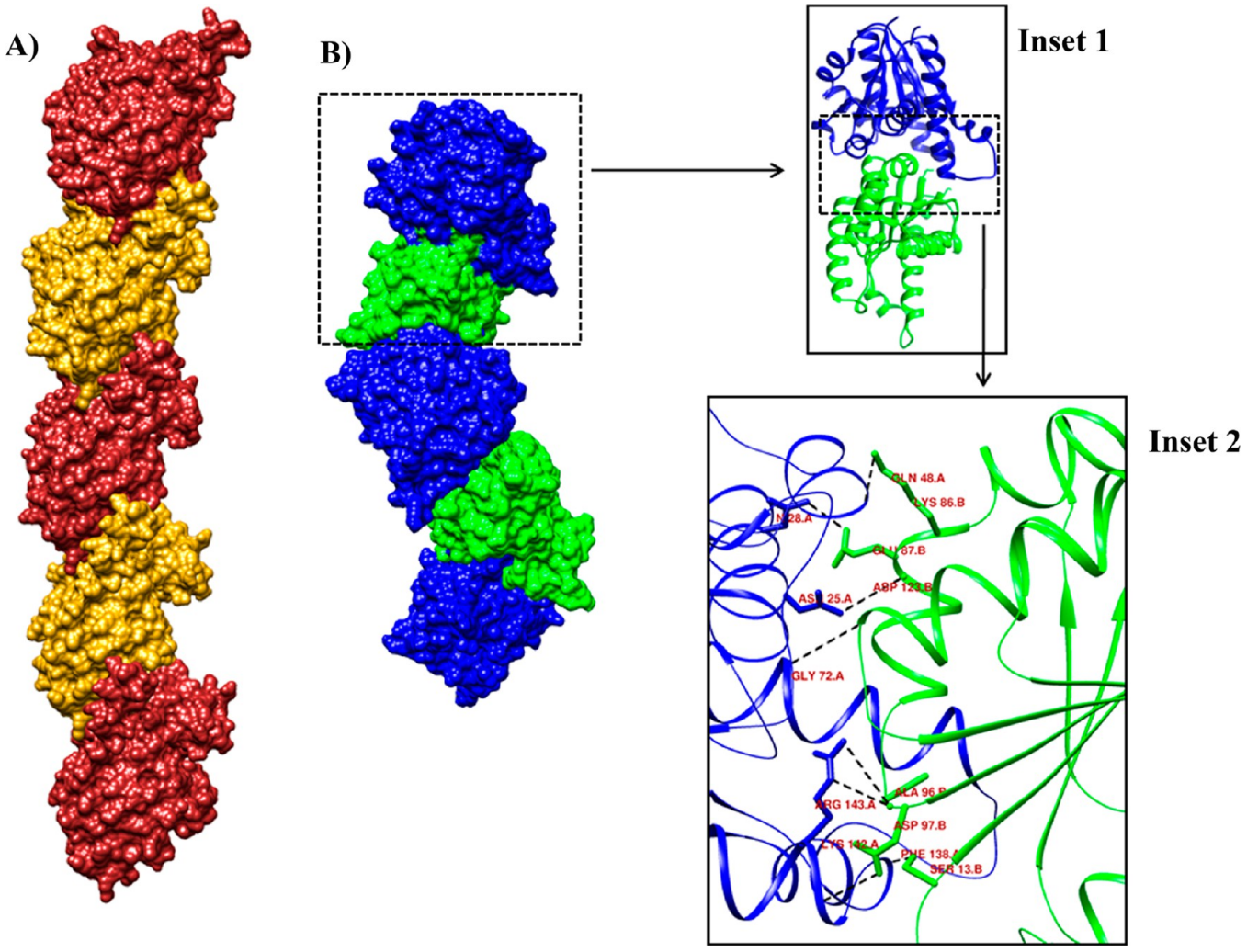

Figure 8. 3D models of protofilaments of FL-FtsZ and the N-domain of FtsZ. (A) 3D model of the FL-FtsZ protofilament (alternating monomers are colored brown and gold). The surface representation of the modeled protofilament is shown. (B) 3D model of the N2-FtsZ protofilament (alternating monomers are colored blue and green). The surface representation of the modeled protofilament is shown. Inset 1 shows the ribbon view of the N2-FtsZ dimer. Inset 2 shows the H-bonding residues between chain A and chain B of the N2-FtsZ dimer. Black dashes show the H-bonds. The models have been constructed from the dimers of FL-FtsZ (PDB entry 1W5A) (A) and the N2 domain of FtsZ (obtained by docking of the N-domain of FtsZ monomers, PDB entry 2VXY) (B). The figures were rendered using UCSF Chimera.[36]

perturbs the lattice structure, causes their dissociation, and increases the GTPase activity of FL-FtsZ. Moreover, C-domains caused a smaller decrease in the polymer mass of FL-FtsZ than the N-domains and did not significantly affect the GTPase activity of FL-FtsZ, indicating that they might just sequester FL-FtsZ monomers to some extent, thereby causing a reduction in the level of polymers of FL-FtsZ.

We made two important observations. The N-domain inhibits the assembly of FL-FtsZ, and the N-domain alone can polymerize in the presence of GTP. An inspection of the 3D model of N-domain filaments indicated that N-domains form slightly curved filaments (Figure 8B). FL-FtsZ is known to form straight protofilaments.[16] The modeled FL-FtsZ protofilament, from the dimer of *M. jannaschii* FtsZ,[16] also exhibited a straight conformation (Figure 8A). This difference in the protofilament structure of FL-FtsZ and the N-domain also provides a possible explanation for the inhibition of FL-FtsZ assembly in the presence of N-domains. Because the geometry of N-domain polymers is different from that of FL-polymers, the incorporation of the N-domain might leave a kink or constraint in the FL-FtsZ protofilaments that weakens the lattice, causing the disassembly of protofilaments.

Furthermore, in a previous study, it was found that the expression of the N-domain is lethal for *E. coli* cells.[13] The study reported that when the N-domain of *E. coli* FtsZ was overexpressed in *E. coli* cells, it led to the inhibition of Z-ring function, whereas overexpression of the C-domain did not perturb the Z-ring. These findings led to the suggestion that the assembly of FtsZ protofilaments could be directional.[13] Accordingly, we found that the expression of N2-FtsZ was toxic to the bacterial cells, and no colonies were obtained while N2-FtsZ construct was being transformed in *E. coli* BL21-(DE3)pLysS cells. The construct could be transformed in *E. coli* C41 cells, which are known to be capable of expressing many toxic proteins.[41] Our *in vitro* experimental observations provide evidence that the N-domain of FtsZ is incorporated into the filaments of FL-FtsZ and causes their disassembly. The inhibition might be due to binding either at the ends or at the lateral regions or both of these regions of growing FL-FtsZ filaments. The data also indicated that N-domains bind to the

dx.doi.org/10.1021/bi400129j | *Biochemistry* 2013, 52, 7071−7081

growing FL-FtsZ polymers, supporting the directional assembly of FL-FtsZ, a mechanism described in the literature.[13]

■ ASSOCIATED CONTENT

Supporting Information

Experimental and theoretical values of the different secondary structure elements of FL-, N1-, and N2-FtsZ (Table S1), polymers of FL-, N1-, and N2-FtsZ after the His tags have been cut (Figure S1), N2-FtsZ inhibiting the polymerization of FL-FtsZ in both PIPES and HEPES buffers (Figure S2), N2-FtsZ inhibiting the polymerization of FL-FtsZ over a wide range of GTP concentrations (Figure S3), N2-FtsZ localizing with the FL-FtsZ filament in PIPES buffer (Figure S4), C-domain constructs of FtsZ inhibiting the polymerization of N1-FtsZ and N2-FtsZ (Figure S5), the possibilities of assembly when N- and C-domains are mixed (Figure S6), and N2-FtsZ inhibiting the polymerization of preformed FL-FtsZ polymers (Figure S7). This material is available free of charge via the Internet at http://pubs.acs.org.

■ AUTHOR INFORMATION

Corresponding Author

*Department of Biosciences and Bioengineering, Indian Institute of Technology Bombay, Mumbai 400076, India. E-mail: panda@iitb.ac.in. Phone: 91-22-2576-7838. Fax: 91-22-2572-3480.

Funding

The work is supported by a grant from the Department of Science and Technology, Government of India.

Notes

The authors declare no competing financial interest.

■ ACKNOWLEDGMENTS

We thank Jayant Asthana for his help with fluorescence and electron microscopy studies.

■ ABBREVIATIONS

FITC, fluorescein isothiocyanate; TRITC, tetramethylrhodamine-5(6)-isothiocyanate; GTP, guanosine 5′-triphosphate; IPTG, isopropyl β-D-1-thiogalactopyranoside; TNP-GTP, 2′,3′-*O*-(2,4,6-trinitrocyclohexadienylidine)guanosine 5′-triphosphate.

■ REFERENCES

(1) Adams, D. W., and Errington, J. (2009) Bacterial cell division: Assembly, maintenance and disassembly of the Z ring. *Nat. Rev. Microbiol. 7*, 642−653.

(2) Löwe, J., and Amos, L. A. (1998) Crystal structure of the bacterial cell-division protein FtsZ. *Nature 391*, 203−206.

(3) Erickson, H. P. (2005) FtsZ, a prokaryotic homolog of tubulin? *Cell 80*, 367−370.

(4) Erickson, H. P., Taylor, D. W., Taylor, K. A., and Bramhill, D. (1996) Bacterial cell division protein FtsZ assembles into protofilament sheets and minirings, structural homologs of tubulin polymers. *Proc. Natl. Acad. Sci. U.S.A. 93*, 519−523.

(5) Tilney, L. G., Bryan, J., Bush, D. J., Fujiwara, K., Mooseker, M. S., Murphy, D. B., and Snyder, D. H. (1973) Microtubules: Evidence for 13 protofilaments. *J. Cell Biol. 59*, 267−275.

(6) Romberg, L., Simon, M., and Erickson, H. P. (2001) Polymerization of FtsZ, a bacterial homolog of tubulin. Is assembly cooperative? *J. Biol. Chem. 276*, 11743−11753.

(7) Kuchibhatla, A., Abdul Rasheed, A. S., Narayanan, J., Bellare, J., and Panda, D. (2009) An analysis of FtsZ assembly using small angle X-ray scattering and electron microscopy. *Langmuir 25*, 3775−3785.

(8) Chen, Y., and Erickson, H. P. (2005) Rapid in vitro assembly dynamics and subunit turnover of FtsZ demonstrated by fluorescence resonance energy transfer. *J. Biol. Chem. 280*, 22549−22554.

(9) Fu, G., Huang, T., Buss, J., Coltharp, C., Hensel, Z., and Xiao, J. (2010) In vivo structure of the *E. coli* FtsZ-ring revealed by photoactivated localization microscopy (PALM). *PLoS One 5*, e12682.

(10) Oliva, M. A., Trambaiolo, D., and Löwe, J. (2007) Structural insights into the conformational variability of FtsZ. *J. Mol. Biol. 373*, 1229−1242.

(11) Romberg, L., and Levin, P. A. (2003) Assembly dynamics of the bacterial cell division protein FTSZ: Poised at the edge of stability. *Annu. Rev. Microbiol. 57*, 125−154.

(12) Redick, S. D., Stricker, J., Briscoe, G., and Erickson, H. P. (2005) Mutants of FtsZ targeting the protofilament interface: Effects on cell division and GTPase activity. *J. Bacteriol. 187*, 2727−2736.

(13) Osawa, M., and Erickson, H. P. (2005) Probing the domain structure of FtsZ by random truncation and insertion of GFP. *Microbiology 151*, 4033−4043.

(14) Vaughan, S., Wickstead, B., Gull, K., and Addinall, S. G. (2004) Molecular evolution of FtsZ protein sequences encoded within the genomes of archaea, bacteria, and eukaryota. *J. Mol. Evol. 58*, 19−29.

(15) Paul, J., Buske, P. J., and Levin, P. A. (2012) Extreme C Terminus of Bacterial Cytoskeletal Protein FtsZ Plays Fundamental Role in Assembly Independent of Modulatory Proteins. *J. Biol. Chem. 287*, 10945−10957.

(16) Oliva, M. A., Cordell, S. C., and Löwe, J. (2004) Structural insights into FtsZ protofilament formation. *Nat. Struct. Mol. Biol. 11*, 1243−1250.

(17) Singh, J. K., Makde, R. D., Kumar, V., and Panda, D. (2007) A membrane protein, EzrA, regulates assembly dynamics of FtsZ by interacting with the C-terminal tail of FtsZ. *Biochemistry 46*, 11013−11022.

(18) Handler, A. A., Lim, J. E., and Losick, R. (2008) Peptide inhibitor of cytokinesis during sporulation in *Bacillus subtilis*. *Mol. Microbiol. 68*, 588−599.

(19) Kuchibhatla, A., Bhattacharya, A., and Panda, D. (2011) ZipA binds to FtsZ with high affinity and enhances the stability of FtsZ protofilaments. *PLoS One 6*, e28262.

(20) Ray, S., Kumar, A., and Panda, D. (2013) GTP regulates the interaction between MciZ and FtsZ: A possible role of MciZ in bacterial cell division. *Biochemistry 52*, 392−401.

(21) Böhm, G., Muhr, R., and Jaenicke, R. (1992) Quantitative analysis of protein far UV circular dichroism spectra by neural networks. *Protein Eng. 5*, 191−195.

(22) Eisenhaber, F., Imperiale, F., Argos, P., and Froemmel, C. (1996) Prediction of Secondary Structural Content of Proteins from Their Amino Acid Composition Alone. I. New Analytic Vector Decomposition Methods. *Proteins 25* (N2), 157−168.

(23) Eisenhaber, F., Froemmel, C., and Argos, P. (1996) Prediction of Secondary Structural Content of Proteins from Their Amino Acid Composition Alone. II. The Paradox with Secondary Structural Class. *Proteins 25* (N2), 169−179.

(24) Jaiswal, R., Beuria, T. K., Mohan, R., Mahajan, S. K., and Panda, D. (2007) Totarol inhibits bacterial cytokinesis by perturbing the assembly dynamics of FtsZ. *Biochemistry 46*, 4211−4220.

(25) Bradford, M. M. (1976) A rapid and sensitive method for the quantitation of microgram quantities of protein utilizing the principle of protein-dye binding. *Anal. Biochem. 72*, 248−254.

(26) Singh, P., Jindal, B., Surolia, A., and Panda, D. (2012) A Rhodanine Derivative CCR-11 Inhibits Bacterial Proliferation by Inhibiting the Assembly and GTPase Activity of FtsZ. *Biochemistry 51*, 5434−5442.

(27) Jaiswal, R., Patel, R. Y., Asthana, J., Jindal, B., Balaji, P. V., and Panda, D. (2010) E93R substitution of *Escherichia coli* FtsZ induces bundling of protofilaments, reduces GTPase activity, and impairs bacterial cytokinesis. *J. Biol. Chem. 285*, 31796−31805.

(28) Geladopoulos, T. P., Sotiroudis, T. G., and Evangelopoulos, A. E. (1991) A malachite green colorimetric assay for protein phosphatase activity. *Anal. Biochem. 192*, 112−116.

(29) Bernstein, F. C., Koetzle, T. F., Williams, G. J., Meyer, E. E., Jr., Brice, M. D., Rodgers, J. R., Kennard, O., Shimanouchi, T., and Tasumi, M. (1977) The Protein Data Bank: A Computer-based Archival File For Macromolecular Structures. *J. Mol. Biol. 112*, 535.
(30) Haydon, D. J., Stokes, N. R., Ure, R., Galbraith, G., Bennett, J. M., Brown, D. R., Baker, P. J., Barynin, V. V., Rice, D. W., Sedelnikova, S. E., Heal, J. R., Sheridan, J. M., Aiwale, S. T., Chauhan, P. K., Srivastava, A., Taneja, A., Collins, I., Errington, J., and Czaplewski, L. G. (2008) An inhibitor of FtsZ with potent and selective anti-staphylococcal activity. *Science 321*, 1673−1675.
(31) Duhovny, D., Nussinov, R., and Wolfson, H. J. (2002) Efficient Unbound Docking of Rigid Molecules. In *Proceedings of the Second Workshop on Algorithms in Bioinformatics (WABI)* (Guigo, R., and Gusfield, D., Eds.) Lecture Notes in Computer Science, Vol. *2452*, pp 185−200, Springer-Verlag, Duesseldorf, Germany.
(32) Schneidman-Duhovny, D., Inbar, Y., Nussinov, R., and Wolfson, H. J. (2005) PatchDock and SymmDock: Servers for rigid and symmetric docking. *Nucleic Acids Res. 33*, W363−W367.
(33) Guex, N., and Peitsch, M. C. (1997) SWISS-MODEL and the Swiss-PdbViewer: An environment for comparative protein modeling. *Electrophoresis 18*, 2714−2723.
(34) *The PyMOL Molecular Graphics System*, version 1.5.0.4 (2010) Schrödinger, LLC, Portland, OR.
(35) Hubbard, S. J., and Thornton, J. M. (1993) *NACCESS*, University College London, London.
(36) Pettersen, E. F., Goddard, T. D., Huang, C. C., Couch, G. S., Greenblatt, D. M., Meng, E. C., and Ferrin, T. E. (2004) UCSF Chimera: A visualization system for exploratory research and analysis. *Comput. Chem. 25*, 1605−1612.
(37) David-Pfeuty, T., Erickson, H. P., and Pantaloni, D. (1977) Guanosinetriphosphatase activity of tubulin associated with microtubule assembly. *Proc. Natl. Acad. Sci. U.S.A. 74*, 5372−5376.
(38) Oxberry, M. E., Geary, T. G., Winterrowd, C. A., and Prichard, R. K. (2001) Individual expression of recombinant α- and β-tubulin from *Haemonchus contortus*: Polymerization and drug effects. *Protein Expression Purif. 21*, 30−39.
(39) Li, Z., Trimble, M. J., Brun, Y. V., and Jensen, G. J. (2007) The structure of FtsZ filaments *in vivo* suggests a force-generating role in cell division. *EMBO J. 26*, 4694−4708.
(40) Makarova, K. S., and Koonin, E. V. (2010) Two new families of the FtsZ-tubulin protein superfamily implicated in membrane remodeling in diverse bacteria and archaea. *Biol. Direct 5*, 33.
(41) Dumon-Seignovert, L., Cariot, G., and Vuillard, L. (2004) The toxicity of recombinant proteins in *Escherichia coli*: A comparison of overexpression in BL21(DE3), C41(DE3), and C43(DE3). *Protein Expression Purif. 37*, 203−206.